J Chem Technol Biotechnol 79:397–402 (online: 2004)
DOI: 10.1002/jctb.996

Extraction of zinc from blast-furnace dust using ammonium sulfate

Hesham I Saleh[1]* and Kamaleldin M Hassan[2]

[1]Department of Inorganic Chemistry, National Research Center, PO 12622, Dokki, Cairo, Egypt
[2]Department of Radioactive Sedimentary Deposits, Nuclear Materials Authority, PO 530, Maadi, Cairo, Egypt

Abstract: The reaction between roasted zinc blast-furnace dust (BFD) and ammonium sulfate was studied in the temperature range 250–450 °C using different molar ratios to determine the maximum extraction of zinc. The reaction products are characterized. The composition of the untreated and roasted BFD, and reaction products was investigated by chemical, thermal, X-ray diffraction and fluorescence analyses. The decomposition of ammonium sulfate leads to the formation of $(NH_4)_2S_2O_7$, NH_4HSO_4 and $(NH_4)_3H(SO_4)_3$. The main zinc reaction products are $ZnSO_4$, $ZnSO_3$, $(NH_4)_2Zn(SO_4)_2$, $(NH_4)_2Zn_2(SO_4)_3$ and $(NH_4)_2Zn_4(SO_4)_5$. The reaction mechanisms of these formations are discussed in detail. The identity of these products depends essentially on the temperature as well as the molar ratios of the reactants. The optimum conditions for the formation of soluble zinc compounds are molar ratio 1:8 of roasted zinc dust (ZnO) and $(NH_4)_2SO_4$ at 350 °C. Under these conditions, up to 95% of zinc was leached with 0.5 M sulfuric acid.

Keywords: blast-furnace dust; ammonium sulfate; reaction products; thermal analysis; zinc recovery

1 INTRODUCTION

Zinc compounds are used as pigments for manufacturing paints, inks, plastics, concretes, glasses and papers,[1] and are also used in medicine and agriculture.[2] The major ores of zinc are ZnS (which is known as zinc blende in Europe and as sphalerite in the USA) and $ZnCO_3$ (calamine in Europe, smithsonite in the USA). Such ores are less common in Egypt. An alternative source of zinc is the blast-furnace dust (BFD) produced during steel–iron-making processes. Studies indicated that the BFD contains up to 60% zinc.[3–5] There are 300 tons of these zinc-rich. Furnace dusts produced monthly in Egypt, which imposes environmental and storage problems (M Shakour, Egyption Iron and Steel Company, personal communication).

Several processes have been developed for extracting zinc compounds from waste and dust materials.[6–13] These include: (a) leaching with NH_3 and NH_4CO_3 or with NH_4SO_4,[8,10] (b) hydrometallurgical leaching with HCl, NaCl, $CaCl_2$, $FeCl_3$ solutions, or their mixtures,[11] (c) fuming process in the presence of coke as a reducing agent,[13] (d) treating with H_2SO_4 followed by NaOH[12] and (e) leaching with acids (H_2SO_4 or HCl).[6,7,9]

The present work was focused on the reaction mechanisms taking place during the interactions between ammonium sulfate and BFD at different temperatures and the recovery of zinc from the reaction products. X-ray, chemical, and thermal analyses were used to characterize the products.

2 EXPERIMENTAL

2.1 Materials

Blast-furnace dust rich in zinc (10 kg) supplied from the Iron and Steel Company, Helwan, Egypt was used in this study. This dust was produced during the steel-iron making process in the company.

2.2 Preparation of reaction mixtures

The supplied sample was finel pulverized to −100 mesh to provide a maximum reacting surface area, and roasted in air at 850 °C for 3h. Five mixtures of roasted zinc dust (ZnO) and $(NH_4)_2SO_4$ with molar ratios 1:1 (I), 1:2 (II), 1:4 (III), 1:6 (IV) and 1:8 (V) were prepared by mixing the reactants, and heating them gradually (10 °C min^{-1}) for 3h to 250, 350 and 450 °C.

2.3 Techniques and measurements

The x-ray diffraction (XRD) analysis of different reaction products was performed using a Philips diffractometer (type PW 1399) employing Fe-filtered CoKα radiation and Ni-filtered CuKα radiation. The X-ray tube was operated at 36 kV and 16 mA and the diffraction angle (2θ) was scanned at a rate of

* Correspondence to: Hesham I Saleh, Department of Inorganic Chemistry, National Research Center, PO 12622, Dokki, Cairo, Egypt
E-mail: hesham1157@yahoo.com
(*Received 2 June 2003; revised version received 12 October 2003; accepted 8 December 2003*)

2 °C min^{-1}. The X-ray fluorescence (XRF) analysis of the zinc dust sample was carried out using a sequential XRF instrument (ARL 9400). Thermal analysis was determined using a Perkin-Elmer thermoanalyzer (Delta series DTA and TG7). A heating rate of 10 °C min^{-1} up to 1000 °C in static air was used in both the DTA and TG measurements.

2.4 Preparation of extract solutions

Weighed samples (0.05 g) of the reaction products were agitated thoroughly in 100 cm^3 of distilled water, and in 100 cm^3 of 0.5 M H_2SO_4 for 30 min followed by filtration. The total volumes of the resulting filtrates were made up to 250 cm^3 and then measured for zinc concentrations using an atomic absorption spectrometer (Spectr AA 220 model, Varian).

3 RESULTS AND DISCUSSION

3.1 Investigation of the studied BFD

The X-ray diffraction patterns of the untreated BFD (Fig 1) indicate the presence of hydrozincite [$Zn_5(CO_3)_2(OH)_6$, $Zn_4(CO_3)(OH)_6{\cdot}H_2O$)], hemimorphite ($Zn_4Si_2O_7(OH)_2{\cdot}H_2O$), smithsonite ($ZnCO_3$), sphalerite (ZnS), gypsum ($CaSO_4{\cdot}2H_2O$), calcite ($CaCO_3$), maghemite (γ-Fe_2O_3), and mullite ($3Al_2O_3{\cdot}2SiO_2$).

The TG and DTA traces (Fig 2) suggest three endothermic and one exothermic effects corresponding to four weight losses: 7.54% at 125 °C, 12.41% at 310 °C, 2.63% at 535 °C and 3% at 825 °C. The total observed weight loss was 25.61%. The first heat event can be attributed to dehydration of gypsum.[14] The second weight loss, observed at 310 °C is associated with the dehydroxylation and decarbonation of

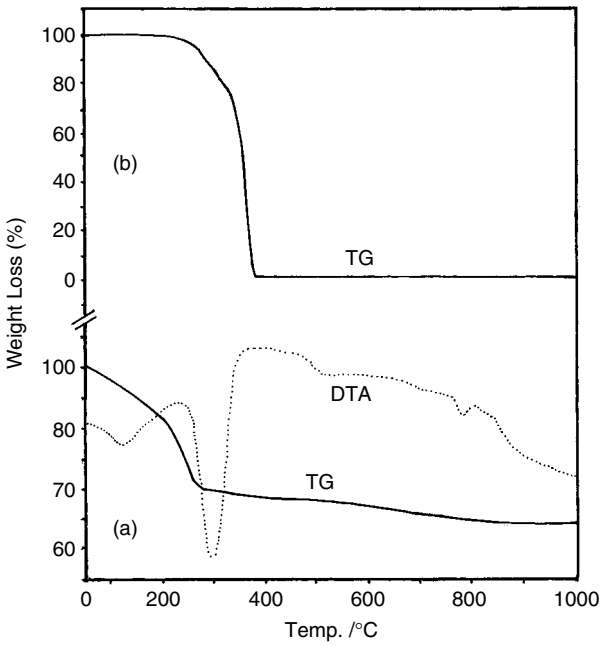

Figure 2. DTA and TG curves of untreated BFD (a) and ammonium sulfate (b).

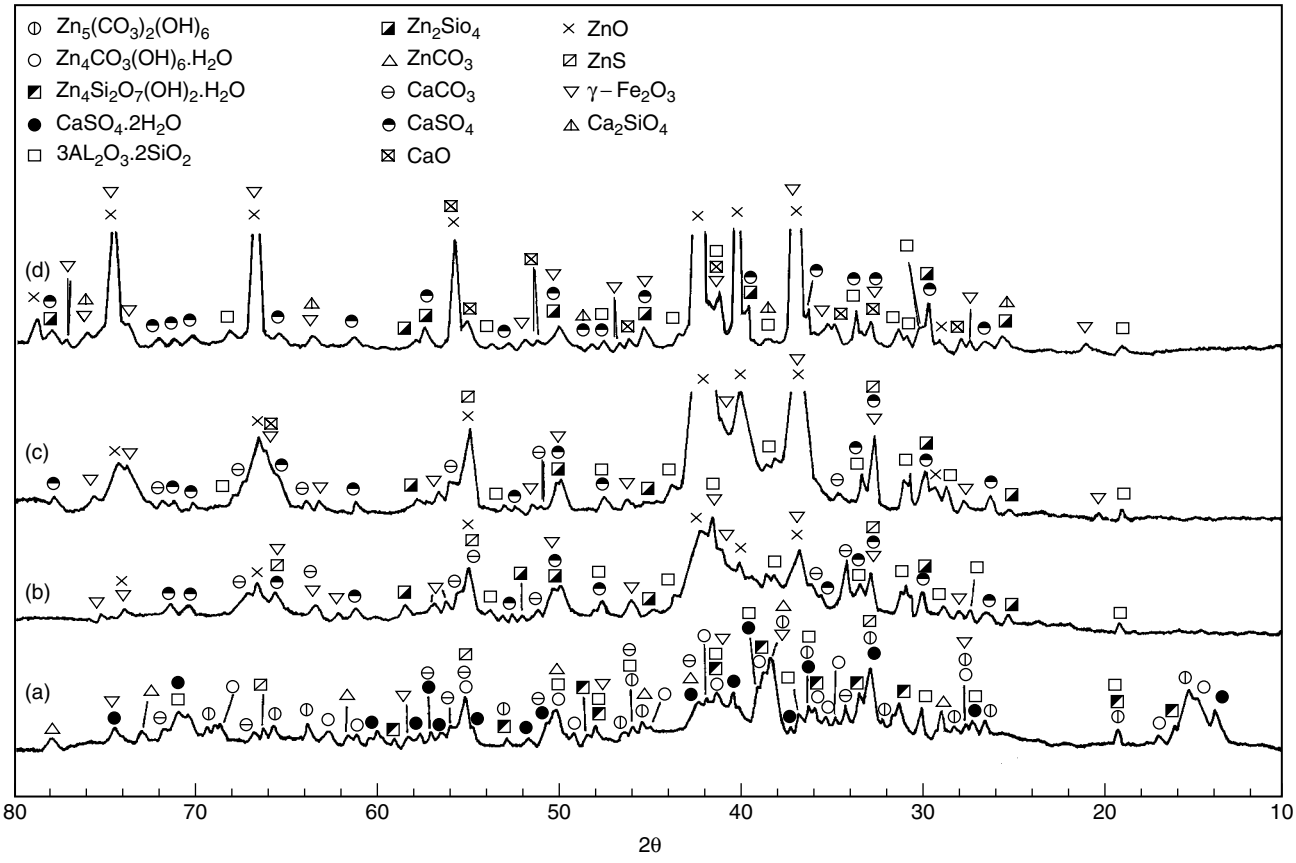

Figure 1. X-ray diffraction patterns of untreated BFD (a) and BFD roasted at 310 °C (b), 525 °C (c), 825 °C (d), for 3 h using CoK $\propto$ radiation and an iron filter.

hydrozincite,[15,16] smithsonite[17] and hemimorphite[18] minerals according to the following equations:

$$Zn_5(CO_3)_2(OH)_6 \xrightarrow{310^\circ C} 5ZnO + 2CO_2 + 3H_2O \quad (1)$$

$$Zn_4(CO_3)(OH)_6.H_2O \xrightarrow{310^\circ C} 4ZnO + CO_2 + 4H_2O \quad (2)$$

$$ZnCO_3 \xrightarrow{310^\circ C} ZnO + CO_2 \quad (3)$$

$$Zn_4Si_2O_7(OH)_2.H_2O \xrightarrow{310^\circ C} 2Zn_2SiO_4 + 2H_2O \quad (4)$$

The above reactions are consistent with the XRD traces for the heated sample at 310 °C (Fig 1), which indicates the absence of hydrozincite, smithsonite and hemimorphite. The third weight loss at 535 °C may be due to the formation of zincite (ZnO) in more crystalline form. This hypothesis was confirmed from the pronounced increase in the peak height of the X-ray diffraction patterns of zincite as the temperature was raised to 535 °C (Fig 1).

The final loss of sample weight, observed at 825 °C, is attributed to the thermal decomposition of sphalerite[19] and calcite[14] as follows:

$$ZnS + 1.5O_2 \xrightarrow{825^\circ C} ZnO + SO_2 \quad (5)$$

$$CaCO_3 \xrightarrow{825^\circ C} CaO + CO_2 \quad (6)$$

This accords with the XRD patterns (Fig 1), which show the presence of CaO and increased intensity of ZnO peaks.

On the basis of these findings the BFD sample was roasted at 850 °C to obtain a more stable Zn form (ZnO) which is more susceptible towards ammonium sulfate attack at low temperatures. The XRD of the roasted BFD at 850 °C (Fig 1) indicates the presence of well developed ZnO as the major phase with small amounts of anhydrite ($CaSO_4$), calcium silicate (Ca_2SiO_4), maghemite (γ-Fe_2O_3), calcium oxide (CaO), willamite (Zn_2SiO_4), and mullite ($3Al_2O_3 \cdot 2SiO_2$).

Chemical analyses of untreated and roasted Zn-rich dust samples by XRF are listed in Table 1.

3.2 Thermal decomposition of ammonium sulfate

The thermal characterization of the reactant ammonium sulfate is considered as a guide that helps in the investigation of the proper reactions which may take place between ammonium sulfate and different constituents of the zinc dust at different temperatures. The thermal decomposition of ammonium sulfate leads to the formation of different reactive species, depending mainly on the thermal treatments.[20,21]

The TG curve of ammonium sulfate (Fig 2) can be subdivided into two steps. These steps range from 220 to 310 °C and from 310 to 375 °C, with weight losses of 17.11 and 81.87%, respectively. The salt was found to lose ammonia and water at 250 °C, forming $(NH_4)_2S_2O_7$ (Table 2), whereas it lost another molecule of ammonia at 300 °C leading to formation of $(NH_4)_3H(SO_4)_2$ and NH_4HSO_4. These findings agree with previous studies,[22–24] and can be represented by the following equations:

$$2(NH_4)_2SO_4 \xrightarrow{250^\circ C} (NH_4)_2S_2O_7 + 2NH_3 + H_2O \quad (7)$$

$$2(NH_4)_2SO_4 \xrightarrow{300^\circ C} 2NH_4HSO_4 + 2NH_3 \quad (8)$$

$$3(NH_4)_2SO_4 \xrightarrow{300^\circ C} NH_4HSO_4 + (NH_4)_3H(SO_4)_2 + 2NH_3 \quad (9)$$

The pyrosulfate is chemically unstable and decomposed at 350 °C (Table 2) to SO_3 and NH_4HSO_4. Its decomposition can be represented by the following equation:

$$(NH_4)_2S_2O_7 \xrightarrow{350^\circ C} NH_4HSO_4 + SO_3 + NH_3 \quad (10)$$

3.3 XRD investigation of the interaction between ammonium sulfate and roasted BFD

The XRD results of the reaction products formed during the interactions between ammonium sulfate and the roasted BFD samples with molar ratios 1:1, 2:1, 4:1, 6:1, and 8:1 at 250, 350, and 450 °C are presented in Table 3. The products were found to depend on the molar ratios and temperatures. At

Table 2. Crystalline phases formed during the thermal decomposition of ammonium sulfate at different temperatures

Temperature (°C)	Crystalline phases
200	$(NH_4)_2SO_4$
250	$(NH_4)_2SO_4$, $(NH_4)_2S_2O_7$
300	$(NH_4)_2S_2O_7$, $(NH_4)_2SO_4$, $(NH_4)_3H(SO_4)_2$
350	NH_4HSO_4, $(NH_4)_3H(SO_4)_2$
400	NH_4HSO_4, $(NH_4)_3H(SO_4)_2$
450	NH_4HSO_4, $(NH_4)_3H(SO_4)_2$ (traces)

Table 1. XRF analysis of untreated and roasted Zn-rich dust samples

	% weight												
Sample	ZnO	CaO	SiO_2	Fe_2O_3	SO_3^-	F	Al_2O_3	MnO	MgO	Cl	K_2O	LOI*	Total
Untreated	49.6	6.58	5.20	4.35	3.01	1.51	3.24	0.33	0.21	0.1	0.06	25.61	99.80
Roasted at 850 °C	59.45	10.80	9.96	8.93	1.46	0.95	6.90	0.70	0.46	—	0.12	—	99.73

*, Loss on ignition.

250 °C ammonium sulfate was partially decomposed into ammonium pyrosulfate (eqn (7)). These species reacted with ZnO in the BFD, forming ammonium zinc sulfate according to the following equations:

$$2(NH_4)_2SO_4 + ZnO \xrightarrow{250^\circ C} (NH_4)_2Zn(SO_4)_2 + 2NH_3 + H_2O \quad (11)$$

$$(NH_4)_2S_2O_7 + ZnO \xrightarrow{250^\circ C} (NH_4)_2Zn(SO_4)_2 \quad (12)$$

The sulfur trioxide resulting from thermal decomposition of ammonium pyrosulfate (Eqn (10)) reacted with zinc oxide found in the BFD and formed $ZnSO_4$, which is consistent with the XRD results of mixture I listed in Table 3. The resulting $ZnSO_4$ reacted instantaneously with the various species of thermal decomposition of ammonium sulfate leading to the formation of different ammonium zinc sulfate[25,26] species at 350 °C (Table 3) according to the following equations:

$$ZnO + SO_3 \xrightarrow{350^\circ C} ZnSO_4 \quad (13)$$

$$ZnSO_4 + 2NH_4HSO_4 \xrightarrow{350^\circ C} (NH_4)_2Zn(SO_4)_2 + H_2O + SO_3 \quad (14)$$

$$2ZnSO_4 + 2NH_4HSO_4 \xrightarrow{350^\circ C} (NH_4)_2Zn_2(SO_4)_3 + H_2O + SO_3 \quad (15)$$

$$4ZnSO_4 + 2NH_4HSO_4 \xrightarrow{350^\circ C} (NH_4)_2Zn_4(SO_4)_5 + H_2O + SO_3 \quad (16)$$

$$ZnSO_4 + (NH_4)_3H(SO_4)_2 \xrightarrow{350^\circ C} (NH_4)_2Zn(SO_4)_2 + H_2O + NH_3 + SO_3 \quad (17)$$

$$2ZnSO_4 + (NH_4)_3H(SO_4)_2 \xrightarrow{350^\circ C} (NH_4)_2Zn_2(SO_4)_3 + H_2O + NH_3 + SO_3 \quad (18)$$

Table 3. The crystalline phases detected in the reaction products for mixtures I–V at different temperatures

	Detected crystalline phases at:		
Mixture	250 °C	350 °C	450 °C
1:1 (I)	a, b, f, g, h, i, k, l, m, p	a, e, f, h, k, l, n	e, f, h, i, k, l, x
1:2 (II)	a, b, f, g, h, i, k, l, m, p	a, b, c, d, e, f, h, k, l, n, o, v, w, z	e, f, h, k, l, x
1:4 (III)	a, b, f, g, h, i, k, l, m, p	b, c, d, h, k, n, o, v, w, z	e, f, h, k, l, x
1:6 (IV)	a, b, f, g, h, i, k, l, m, p	b, c, d, h, k, n, o, v, w, z,	e, f, h, k, l, x
1:8 (V)	a, b, f, g, h, i, k, l, m, p	b, c, d, h, k, n, o, v, w, z,	e, f, h, k, l, x

(a) $(NH_4)_2Zn(SO_4)_2$, (b) $(NH_4)_2Zn(SO_4)_2{\cdot}6H_2O$, (c) $(NH_4)_2Zn_4(SO_4)_5$, (d) $(NH_4)_2Zn_2(SO_4)_3$, (e) $ZnSO_4$, (f) $CaSO_4$, (g) CaO, (h) $ZnSiO_4$, (i) ZnO, (k) $3Al_2O_3{\cdot}SiO_2$, (l) γ-Fe_2O_3, (m) $(NH_4)_2SO_4$, (n) NH_4HSO_4, (o) $(NH_4)_3H(SO_4)_2$, (p) $(NH_4)_2S_2O_7$, (v) $ZnSO_3$, (w) $(NH_4)_2SO_4{\cdot}Fe_2(SO_4)_3$, (x) $Fe_2(SO_4)_3$, (z) $(NH_4)_2Ca_2(SO_4)_3$.

$$4ZnSO_4 + (NH_4)_3H(SO_4)_2 \xrightarrow{350^\circ C} (NH_4)_2Zn_4(SO_4)_5 + H_2O + NH_3 + SO_3 \quad (19)$$

At the same temperature (350 °C), $ZnSO_3$ was also detected (Table 3), which was probably formed as a result of the evolution of SO_2 from SO_3 reduction by ammonia.[27] In addition $(NH_4)_2Ca_2(SO_4)_3$[28] and $(NH_4)_2SO_4{\cdot}Fe(SO_4)_3$[22] were also formed in the reaction mixtures, specially when the ammonium sulfate concentration increased (Table 3). The mechanisms suggested for the formation of these species are shown below:

$$3NH_4HSO_4 + 2CaO \xrightarrow{350^\circ C} (NH_4)_2Ca_2(SO_4)_3 + NH_3 + 2H_2O \quad (20)$$

$$4NH_4HSO_4 + 0.5Fe_2O_3 \xrightarrow{350^\circ C} (NH_4)_2SO_4 \cdot Fe(SO_4)_3 + 2NH_3 + 1.5H_2O \quad (21)$$

$$2(NH_4)_3H(SO_4)_2 + 2CaO \xrightarrow{350^\circ C} (NH_4)_2Ca_2(SO_4)_3 + 4NH_3 + SO_3 + 3H_2O \quad (22)$$

$$2(NH_4)_3H(SO_4)_2 + 0.5Fe_2O_3 + 0.75O_2 \xrightarrow{350^\circ C} (NH_4)_2SO_4 \cdot Fe(SO_4)_3 + 4NH_3 + 3H_2O \quad (23)$$

On raising the temperature to 450 °C, $ZnSO_4$, $CaSO_4$ and $Fe_2(SO_4)_3$ were formed in all mixtures (Table 3). Their formations are probably due to the thermal decomposition of ammonium zinc,[25,26] calcium,[29] and iron sulfates[22] respectively.

3.4 Extraction of zinc from the roasted BFD

The interaction between the BFD and ammonium sulfate therefore results in the production of several zinc compounds, which can be extracted by means of cold water and 0.5 M H_2SO_4. The percentage of zinc extraction increased from 66% to 95% with increasing the molar ratio between reactants. It was also increased by elevating the reaction temperature from 250 °C to 350 °C, followed by a pronounced decrease at higher temperatures (Fig 3). The percentage of zinc in the water and acid extractants increased from 18 to 73% and from 65 to 95%, respectively (Fig 3). The decrease in the extraction efficiency observed at 450 °C is probably due to the formation of $ZnSO_4$, which is less soluble than the $(NH_4)_2Zn(SO_4)_2$, $(NH_4)_2Zn_2(SO_4)_3$, and $(NH_4)_2Zn_4(SO_4)_5$ formed at lower temperatures. The amount of Zn extracted by distilled water is less than that extracted by 0.5 M H_2SO_4. This may be attributed to differences in the solubilities of zinc compounds.

3.5 Recovery of zinc as hydroxide

The dust (15 g) was mixed with 97.2 g of ammonium sulfate, with molar ratio ZnO: $(NH_4)_2SO_4$ of 1:8. The product mixtures (98.45 g) formed at 350 °C/3 h were added to 500 cm^3 of 0.5 M H_2SO_4, stirred,

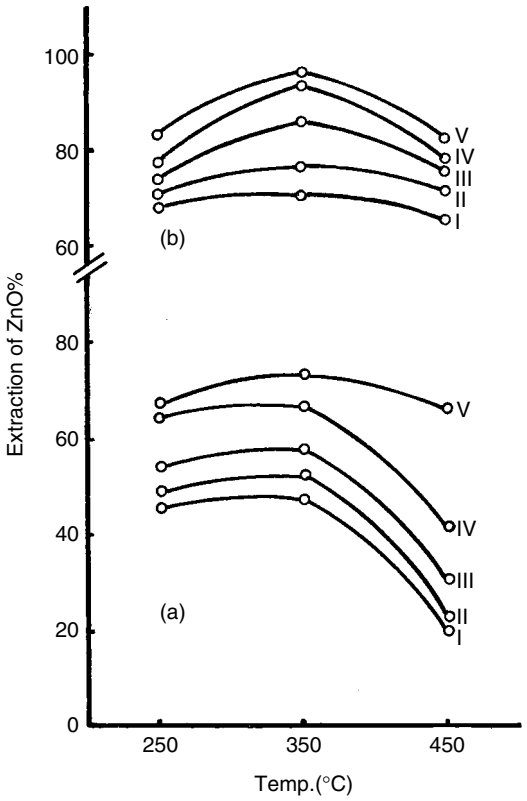

Figure 3. Effect of reaction temperatures on the extraction of zinc from reaction mixture products of roasted BFD and ammonium sulfate with molar ratios 1:1 (I), 1:2 (II), 1:4 (III), 1:6 (IV), and 1:8 (V) by cold water (a) and 0.5 M H_2SO_4(b).

left for 2 h, and then filtered to yield an insoluble precipitate (2.73 g). This precipitate is composed of ZnO, Zn_2SiO_4, CaO, Ca_2SiO_4, $3Al_2O_3{\cdot}2SiO_2$ and Fe_2O_3 (Fig 4(a)). The filtrate (pH = 1.64) was treated with 48 cm^3 of ammonia solution (25% NH_3), which raised the pH to 5.5 and resulted in the precipitation of undesirable impurities. These impurities weighed 5.56 g and include aluminum, iron, calcium hydroxides and calcium sulfate, which were confirmed by XRD analysis (Fig 4(b)). The pH of the filtrate was raised to 7 by adding 27 cm^3 of NH_3 solution. This resulted in the formation of a white precipitate (9.5 g), which was dried at 70 °C for 3 h. The precipitate was examined by XRD and found to consist of $Zn(OH)_2{\cdot}0.5H_2O$ (Fig 4(c)). This agrees with previous studies.[30] The residual solution was concentrated prior to crystallization where ammonium sulfate (40 g) was obtained in a pure form (Fig 4(d)).

CONCLUSIONS

(1) The untreated BFD consists mainly of hydrozincite, hemimorphite, smithsonite, and sphalerite while the roasted BFD at 850 °C includes zincite with small quantities of willamite.

(2) The thermal analysis of the BFD suggests a four-step process corresponding to the (i) dehydration of gypsum, (ii) dehydroxylation and decarbonation of hydrozincite, hemimorphite, and smithsonite, (iii) formation of zincite, and (iv)

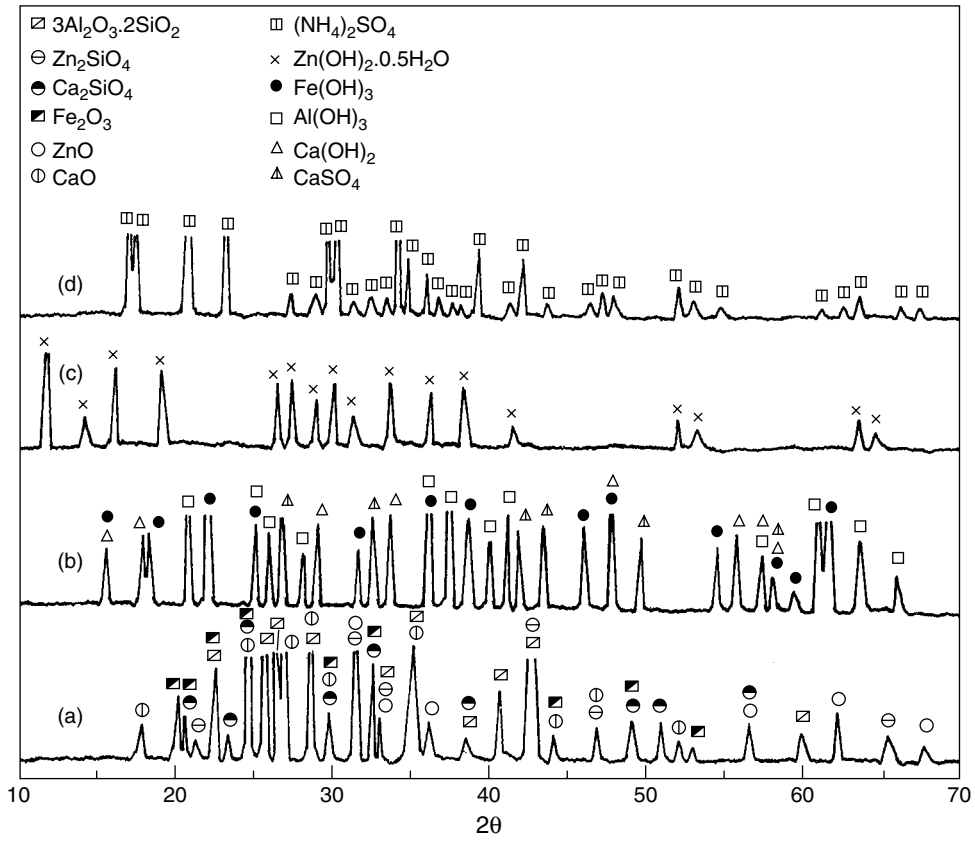

Figure 4. X-ray diffraction patterns of different precipitates from the reaction products treated with ammonium solution at different pH values: (a) insoluble materials, (b) undesirable impurities at pH = 5.5, (c) zinc hydroxide, at pH = 7.0 and (d) ammonium sulfate.

thermal decomposition of sphalerite and calcite, respectively.

(3) $(NH_4)_2Zn(SO_4)_2$, $(NH_4)_2Zn_2(SO_4)_3$, $(NH_4)_2Zn_4(SO_4)_5$, $ZnSO_4$, and $ZnSO_3$ were formed during the interactions between ammonium sulfate and roasted BFD depending on molar ratios and temperatures.

(4) The maximum extraction of zinc as hydroxide was 95% using 0.5 M H_2SO_4 and 73% with distilled water.

REFERENCES

1 Paulette T, Pigments manufactured from minerals. Can Patent 2, 186, 964 (1998).

2 Sonnenwirthy AC and Jarett L, *Gradwohl's Clinical laboratory Methods and Diagnosis*. CV Mosby Company, Copyright, London, pp 376–378 (1980).

3 Pinaev AK, Glazov AN, Tolstoguzov NV and Kachurin DS, Processing of sludge from blast-furnace gas purification. *USSR Stal'* **11**:1056–1057 (1972).

4 Jensen CW, Smelting mixed flue dust. *Mining Mag* **82**:211–214 (1950).

5 Frishberg IV, Gribovskii SV, Korepanova ES and Okunev AI, Preparation of zinc powder during the metallothermal reduction of zincous raw-material. *Izv Akad Nauk SSSR, Metal* **4**:53–55 (1973).

6 Guo-Jun W, Manufacturing technology of activated zinc oxide from the lead-zinc oxide mineral. *Huaxue Gongye Yn Gongcheng* **1**7:37–42 (2000) (in Chinese).

7 Heikki T, Leaching of zinc concentrates at Outokumpu Kokkola plant, Finland. *Schriftenr GFMB* **82**:129–138 (1998).

8 Jingang W, Manufacture of active zinc oxide. Ch patent 1,276,343 (2000).

9 Gotthard B, Metal material useful in refining processes. *Tek Tidskr* **105**:4–25 (1975).

10 Anand S, Rao KS and Das RP, Process development for extraction of zin, copper, and lead from complex sulfide ore/concentrate. Part V: Kinetics of dissolution of copper minerals during ammoniacal leaching of complex sulfide concentrate. *Trans Indian Inst Met* **39**:51–56 (1986).

11 Dobrescu L, Visan S, Socolescu A, Botez L, Iordachescu G and Pop A, Hydrometallurgical recovery of copper and zinc from complex sulfides and oxides. *Mine Pet Gaze Rom* **37**:367–371 (1986).

12 Kiyoshi S, Recovering zinc and lead from dust generated from steelmaking furnaces. Jpn patent 74 59,004 (1974).

13 Kivoshi A, Sakichi G, Ryuzo S and Masao F, Fuming of zinc—bearing slags. *Nippon Kogyo Kaishi*. **84**:1597–1602 (1968). (in Japanese).

14 Paulik F, Paulik J and Erdey L, A complex method in thermal analysis. *Talanta* **13**:1405–1430 (1966).

15 Feitnecht W and Oswald HR, Zn hydroxide carbonates. *Helv Chim Acta* **49**:334–344 (1965).

16 Utsugi H and Tamiya K, Pore structure of zinc oxide prepared from basic zinc carbonate. *Nippon Kagaku Zasshi* **86**:699–704 (1965).

17 Weast RC and Astle MJ, *CRC Handbook of Chemistry and Physics*, 62 nd edn. Library of Congress, USA, pp 164–165 (1981).

18 Roberts WL, Rapp GR and Weber J, *Encyclopedia of Minerals*. Van Nostrand Reinhold Company, New York, pp 267–268 (1974).

19 Lefevre M, Lemmerling J and Tiggelen AV, Some reactions in the roasting of precipitated sulfides. *Bull Soc Chim Belges* **65**:580–595 (1956).

20 Fouda MFR, Amin RS and Abd Elzaher MM, Characterization of products of interaction between kaoline ore and ammonium sulphate. *J Chem Technol Biotechnol* **56**:195–202 (1993).

21 Rafal'skii NG and Ostrovkaya LE, Kinetics and mechanism of the thermal decomposition of ammonium sulfate. *Geterogennye Reaktsii Reakts Sposobnost (USSR)* **Sb**:95–101 (1964).

22 Hidetsugu N, Yasutake H and Hideyo O, Studies on reactions of ammonium sulfate with metallic oxides. 1. The thermal decomposition of ammonium sulfate and its reaction with iron (III) oxide. *Jpn Nippon Kagaku, Kaishi* **5**:706–710 (1980).

23 Konkoly TI, DSC studies of binary inorganic ammonium compound systems. *J Thermal Anal* **27**:275–286 (1983).

24 Sooryanarayana K, Row TN and Robinson WT, Phase transitions, in triammonium hydrogen disulphate. Crystal structure of an intermediate stable phase at −90°. *Phase Transitions* **69**:429–438 (1999).

25 Rocchiccioli C, Thermogravimetry and infrared absorption spectrography of several double sulfates of the magnesium series. I. Thermolysis curves *Mikrochim Ichnoanal Acta* **2–4**:234–237 (1964).

26 Michele T and Joseph T, Thermal evolution of schoenite, $(NH_4)_2Zn(SO_4)_2{\cdot}6H_2O$. *CR Acad Sci*. **272**:400–402 (1971) (in French).

27 Appel R and Huber W, Reaction between sulfur trioxide and ammonia. *Chem Ber* **89**:386–393 (1956).

28 Natl Bur Stand (USA), *Monogr* No 25, p 87–88 (1970).

29 Sahoo PK, Bose SK, and Sircar SC, Sulfation of aluminum oxide, calcium oxide, cadmium oxide, and zinc oxide with ammonium sulfate. *Thermochim Acta* **31**:315–322 (1979).

30 Vogel A and Bassett J, *Textbook of Quantitative Inorganic Analysis*, 4th edn. ELBS English Book Society/Longman, Harlow, pp 135–137 (1978).